ELSEVIER

www.elsevier.nl/locate/jorganchem

Journal of Organometallic Chemistry 587 (1999) 221–232

Journal of Organometallic Chemistry

Haptotropic shifts in organometallic complexes with η^5-coordinated π ligands

Luis F. Veiros *

Centro de Química Estrutural, Instituto Superior Técnico, 1049-001 Lisboa, Portugal

Received 20 April 1999

Professor Maria José Calhorda.

Abstract

The electronic structure and bonding of a series of tricarbonylmanganese complexes, $[(\eta^n\text{-X})Mn(CO)_3]^m$, were studied by means of ab initio calculations using the B3LYP hybrid functional with a LANL2DZ basis set. The following complexes with hydrocarbon ligands were addressed ($n = 5$, $m = 0$): X = cyclopentadienyl ($Cp = C_5H_5^-$), indenyl ($Ind = C_9H_7^-$), fluorenyl ($flu = C_{13}H_9^-$), cyclopenta[*def*]phenanthrenyl ($cpp = C_{15}H_9^-$), 8-hydro-*as*-indacene (*as*-ind = $C_{12}H_9^-$) and 5-hydro-*s*-indacene (*s*-ind = $C_{12}H_9^-$). Two complexes with heterocyclic ligands, X = pyrrolyl ($pyr = NC_4H_4^-$, $n = 5$, $m = 0$) and X = thiophene ($tp = SC_4H_4$, $n = 5$, $m = 1+$) were also studied. For all those species, in which X is a η^5-coordinated π ligand, the bonding was analysed, and the optimised structures were compared with the experimentally determined X-ray structures, available from the literature. The results show a weakening of the (η^5-X)–Mn bond with the increasing of the ligands π system extension. The η^3 species resulting from a two electrons reduction of the previous complexes were studied, their structures optimised, and a comparison between the different coordination geometries of η^3-X is provided. Thus, for the fluorenyl and cyclopenta[*def*]phenanthrenyl complexes, an *exo*cyclic allylic coordination was found for the reduced species ($n = 3$, $m = 2-$). For the indenyl and indacene reduced complexes two possible coordination geometries were studied, the *exo*cyclic and the folded η^3-X, the latter being found the more stable for all these species (X = Ind, *as*-ind, *s*-ind; $n = 3$, $m = 2-$). The heterocyclic ligands were shown to adopt a σ rather than a η^3 coordination geometry, in the corresponding reduced complexes ($m = 2-$ for pyr and $m = 1-$ for tp).

Keywords: Haptotropic shifts; Ring-slippage; Ring-folding; Tricarbonylmanganese; Molecular orbital calculations

1. Introduction

Haptotropic shifts of coordinated polyenic ligands are well-known processes by which a metal centre adjusts its total electron count upon addition or removal of ligands or electrons. When cyclic polyenic ligands are concerned this process is casually termed 'ring-slippage', and has been reviewed for the cyclopentadienyl (Cp) and indenyl (Ind) ligands [1]. These rearrangements play a very important role in substitution reactions, as the reaction rate is often related to the ease of the haptotropic shift. In fact, a remarkable rate acceleration is observed in substitution reactions with $[(Ind)ML_n]$ complexes, when compared with their Cp analogues — the indenyl effect [2], being detected in a number of catalytic reactions [3–9]. This effect grows with the increasing of the ligand's π system extension, as is shown by comparing the activation energies of substitution reactions of fluorenyl (flu), with indenyl and cyclopentadienyl complexes [10].

Given the importance of those substitution reactions, e.g. in catalytic processes, the renewed interest in the study and characterisation of species with η^3 coordinated polyenic ligands is easily understandable. In fact, these may be used as models for reaction intermediates that in most practical cases can only be postulated. A number of polyenic ligands have been the subject of these studies, as shown from a Cambridge Structural Data Base (CSD) [11] survey. The coordination modes discussed in this work are presented in Scheme 1 for selected representative ligands.

* Tel.: +351-1-8419283; fax: +351-1-8464455.
E-mail address: veiros@ist.utl.pt (L.F. Veiros)

0022-328X/99/$ - see front matter
PII: S0022-328X(99)00327-7

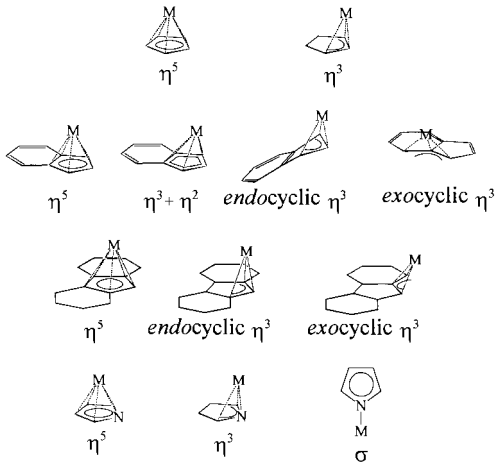

Scheme 1.

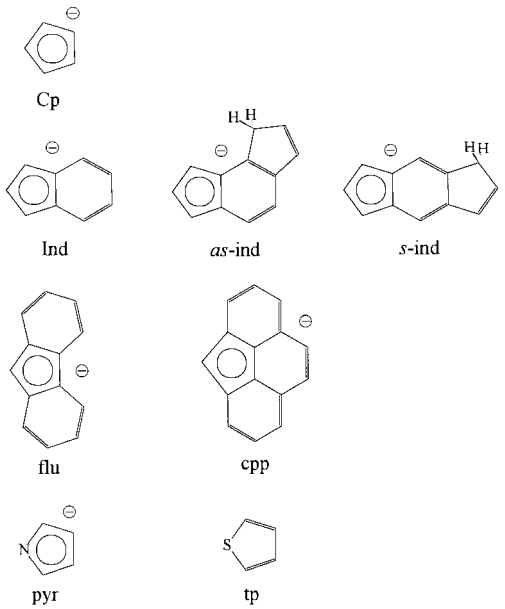

Scheme 2.

Although comparatively rare, η^5 to η^3 shifts have been reported for Cp complexes, the final η^3-Cp complex being characterised in solution [12] or in the solid state [13]. On the other hand, the ligand most widely studied is certainly indenyl. Reduction by two electrons has been shown to induce η^5 to η^3 shifts in systems such as $[(\eta^5\text{-Ind})_2V(CO)_2]$ [14], $[(\eta^5\text{-Ind})CpMoL_2]^{2+}$ [15–18], $[(\eta^5\text{-Ind})Mn(CO)_3]$ [19] or $[(\eta^5\text{-Ind})(\eta^4\text{-cod})Rh]$ [20]. Addition of a ligand can also result in indenyl slippage, as reported for $[(\eta^5\text{-Ind})Mo(CO)_2L_2]^{2+}$ [21]. Many other η^3-indenyl derivatives were structurally characterised, detected or postulated as intermediates in several substitution reactions [22–32]. The different Ind-M coordination modes (see Scheme 1) were systematised and geometrical parameters developed [33], which are often related with NMR results regarding the hapticity of indenyl complexes in solution [34–38].

The η^3 *exo*cyclic coordination mode has been pointed as the intermediate for ring-slippage reactions involving ligands with more extended π systems, such as fluorenyl or cpp (cpp = cyclopenta[*def*]phenanthrenyl) complexes [24,39–42], but a full structural characterisation has only been accomplished for some fluorenyl complexes [43–45].

Since the pioneer article by Hoffmann and co-workers [46], a large amount of work has been published on the theoretical understanding of the bonding and ring slippage in polyenic complexes. Although some dealt with larger ligands such as fluorenyl or cpp [41,42,45], most concerned Cp or indenyl complexes, studying the ligand bonding and their possible hapticities [47–52] or specifically addressing the indenyl effect [16–18,21,53,54].

This work presents a comparative study on a series of tricarbonylmanganese polyenic complexes, by means of ab initio molecular orbitals calculations. The metallic fragment chosen, $Mn(CO)_3$, presents a great number of Mn(I) η^5 polyenic complexes, $[(\eta^5\text{-X})Mn(CO)_3]^m$, with full structural characterisation [11], but, to our knowledge, there are no experimental X-ray structures determined for the η^3 intermediates resulting from a two-electron reduction of these species. Thus, geometry optimisations of the η^5 complexes are presented, and the results are compared with the published X-ray structures, in order to test the theoretical model used. Different possible coordination geometries of the polyenic ligand on the η^3 intermediates are compared and, for each case, the bonding and electronic structure of these species are discussed and complemented with the orbital analysis provided by the extended Hückel method [55,56] (see Appendix for computational details). The following complexes with polyenic hydrocarbon ligands are presented ($m = 0$): X = cyclopentadienyl ($Cp = C_5H_5^-$), indenyl ($Ind = C_9H_7^-$), fluorenyl ($flu = C_{13}H_9^-$), cyclopenta[*def*]phenanthrenyl ($cpp = C_{15}H_9^-$), 8-hydro-*as*-indacene (*as*-ind = $C_{12}H_9^-$) and 5-hydro-*s*-indacene (*s*-ind = $C_{12}H_9^-$). Two heterocyclic ligands are also addressed: pyrrolyl ($pyr = NC_4H_4^-$, $m = 0$) and thiophene ($tp = SC_4H_4$, $m = 1+$). The ligands, X, studied in this work are depicted in Scheme 2 grouped by their geometrical complexity and π-system characteristics, namely: simple Cp, in which the entire π system binds to the metal, when η^5-coordinated; indenyl and indacene ligands, with only one benzene fused to the binding C_5 pentagon, thus maintaining the C_5 ring flexibility; the larger flu and cpp ligands, with two and three fused benzenes, and consequently a more rigid binding C_5 ring; and the two heterocyclic ligands, pyrrolyl and thiophene.

2. Results and discussion

2.1. Complexes with η^5-coordinated polyenic ligands, $[(\eta^5\text{-X})Mn(CO)_3]$

The bonding of a cyclic π ligand η^5 coordinated to a metal centre has been well known for a long time [57], being qualitatively similar for all the hydrocarbon ligands studied in this work (Scheme 2). A simplified representation of the orbital interactions involved for the cyclopentadienyl complex, $[(\eta^5\text{-Cp})Mn(CO)_3]$, is presented in Fig. 1 in which the notation of Refs. [53,54] is used, 's' and 'a' meaning symmetrical or antisymmetrical with respect to the plane of a C_s or pseudo-C_s symmetry such as the one used throughout this work (see Appendix for details).

The $(\eta^5\text{-X})$–M bond results from three orbital interactions, one with σ symmetry and two with π character. The σ component is a three orbital interaction, being a combination of metal z and z^2 orbitals (empty and filled, respectively) with the more stable, symmetrical, ligand π orbital ($1\pi_s$ in Fig. 1). From this interaction result three molecular orbitals, a filled bonding orbital (σ in Fig. 1), which is essentially ligand $1\pi_s$, the high-energy antibonding counterpart, σ* (empty, not represented in Fig. 1) with mainly metal z character, and the complex highest occupied molecular orbital (HOMO), which ends up being essentially metal z^2. The two π interactions, π_s and π_a, are combinations of ligand filled π orbitals with appropriate nodal characteristics (e_1'' in the case of Cp) with the two metal d orbitals with the right symmetry, pointing towards the ligand (xz and yz in Fig. 1). These result in two filled bonding orbitals and the corresponding empty antibonding ones, π_s^* and π_a^*, which constitute the group of the complex lowest unoccupied molecular orbitals (LUMOs). The two metal d orbitals parallel to the ligand X plane (xy and x^2-y^2 in Fig. 1) remain essentially nonbonding. The overall $(\eta^5\text{-X})$–M bonding is, thus, the result of three X to M two-electron donations.

Although qualitatively similar and resulting from the three interactions discussed above, the $(\eta^5\text{-X})$–M bond presents some differences, according to the polyenic ligand, X, involved, as suggested by a survey of the published X-ray structures for $[(\eta^5\text{-X})Mn(CO)_3]$ [11]. In fact, the differences in energies and nodal characteristics of the ligand's X π orbitals relevant for the bonding to the metal ($1\pi_s$, $2\pi_s$ and $1\pi_a$) produce changes that can be seen from structural parameters such as bond distances and angles. This has been extensively discussed in a previous work [54] for the differences between η^5-Cp and η^5-Ind complexes.

An evaluation of the theoretical model used here for the study of the electronic structure of the $[(\eta^5\text{-X})Mn(CO)_3]$ complexes was accomplished by means of the geometry optimisation for each case, and the comparison of the results with the published X-ray structure for the real complex. The two extreme conformations, resulting from the relative orientation of the X ring to the CO ligands, were analysed, as depicted in Scheme 3 for a general ligand X: one in which an apex carbon from the bonding C_5 ring (C_a in Scheme 3) is eclipsed with a carbonyl ligand conforma-

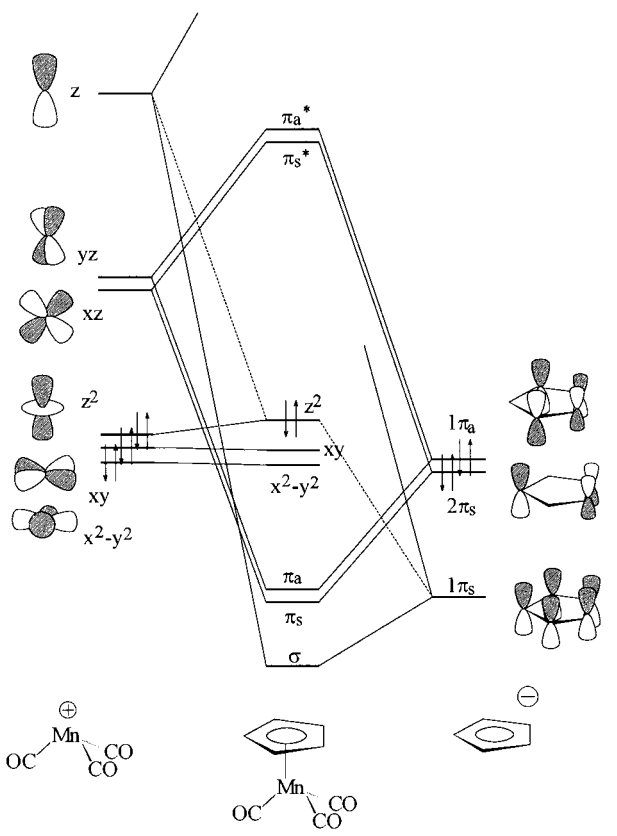

Fig. 1. Schematic representation of the $(\eta^5\text{-X})^-$–$[Mn(CO)_3]^+$ bond for $[(\eta^5\text{-Cp})Mn(CO)_3]$.

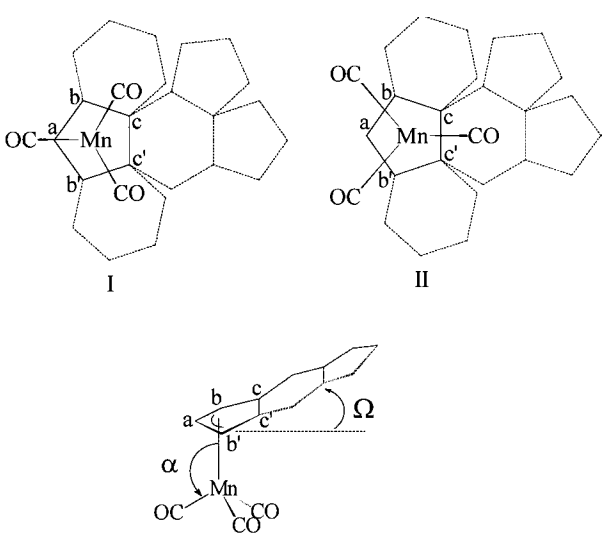

Scheme 3.

Table 1
Structural parameters for the optimised geometries of $[(\eta^5\text{-X})Mn(CO)_3]^m$ complexes (distances in Å and angles in °) [a]

X (m) [Ref.]	Mn–C(CO)	C–O	Mn–C_a/N/S	Mn–$C_{b,b'}$	Mn–$C_{c,c'}$	Ω	α	Conf	$\Delta E_{I/II}$/eV	Refcode
Cp ($m=0$)	1.790	1.181	2.225	2.221	2.223	~0	123	I	0.00	
Cp [58]	*1.788–1.797*	*1.137–1.148*	*2.138*	*2.136;2.142*	*2.133;2.141*	*~0*	*123–124*	*I*		*CPMNCO02*
Ind ($m=0$)	1.792	1.181	2.193	2.199	2.326	8	123	I	0.16	
BrInd [59] [b]	*1.780–1.817*	*1.130–1.161*	*2.131*	*2.124;2.127*	*2.205;2.223*	*4*	*124*	*I*		*BINCMN*
as-ind ($m=0$)	1.791	1.182	2.188	2.196	2.324	7	123	I	0.16	
Me_2-as-ind [60] [b]	*1.771–1.805*	*1.117–1.148*	*2.143;2.147*	*2.134–2.158*	*2.185–2.200*	*7*	*121–126*	*I*		*GEKRET*
s-ind ($m=0$)	1.791	1.182	2.188	2.196	2.335	8	123	I	0.16	
s-ind [61]	*1.177–1.801*	*1.144–1.152*	*2.107*	*2.123;2.128*	*2.210;2.217*	*4*	*122–124*	*I*		*FEHHAB*
flu ($m=0$)	1.793	1.181	2.208	2.257	2.336	–	123	II	0.14	
Phflu [62] [b]	*1.777–1.816*	*1.142–1.162*	*2.154*	*2.194*	*2.206;2.211*	–	*122–125*	*II*		*ZULKOG*
cpp ($m=0$)	1.793	1.181	2.186	2.281	2.333	–	124	II	0.08	
cpp [41]	*1.778–1.801*	*1.140–1.148*	*2.120*	*2.204;2.205*	*2.202;2.210*	–	*123–125*	*II*		*PESFUU*
pyr ($m=0$)	1.794	1.179	2.217	2.217	2.244	2	123	II	0.07	
Me_2pyr [63] [b]	*1.760–1.800*	*1.127–1.157*	*2.109;2.119*	*2.089–2.107*	*2.173–2.196*	*8*	*123–126*	*II*		*FIBHUT*
Me_4pyr [64] [b]	*1.618–1.873*	*1.072–1.226*	*2.102;2.121*	*2.081–2.142*	*2.134–2.196*	*5*	*122–126*	*II*		*WIJNUY*
tp ($m=1$)	1.820	1.168	2.540	2.267	2.376	8	125	II	0.38	
$[Cr(CO)_5]$tp [65] [b]	*1.805–1.820*	*1.127–1.140*	*2.330*	*2.131;2.299*	*2.150;2.253*	*3*	*121–126*	*II*		*PEGGOX*
$[CrMn(CO)_{10}]$ tp [66] [b]	*1.743–1.800*	*1.115–1.173*	*2.319*	*2.230;2.304*	*2.136;2.151*	*2*	*121–127*	*II*		*HANZAX*

[a] Experimental values from X-ray crystal structures are given in italic with the CSD REFCODE and Ref.
[b] X-ray structures only available for substituted R_nX ligands.

tion I, and the other with all the C_5 carbons alternating with the CO ligands conformation II. The structural parameters used to characterise the X ligands hapticipty are the five Mn–C_x distances (x = a, b, b′, c, c′) and the folding angle, defined as the angle between the planes of C_a, C_b, $C_{b'}$, and C_b, $C_{b'}$, C_c, $C_{c'}$, respectively (this corresponds to angle Ω used in reference [33] to characterise the folding in indenyl complexes).

The more relevant structural parameters obtained with the geometry optimisations of the $[(\eta^5\text{-X})Mn(CO)_3]$ complexes are compiled in Table 1, with values taken from the X-ray structural determinations, their references and CSD refcodes. The more stable conformation, relative to the X–CO orientation (I or II, in Scheme 3) is compared with the crystal structure, and the energy difference between optimised I and II is also presented.

The values of Table 1 show a fairly good agreement between the optimised geometries and the published crystal structures, thus supporting the theoretical approach used. This is specially true if it is taken into account that the published structures for five out of the eight complexes studied correspond to substituted polyenic ligands, with the consequently distorted geometries and symmetry break. Consequently, the values obtained for the optimised Mn–C_5 and C–O bond distances are slightly longer than the corresponding experimental values.

For the cyclopentadienyl complex $[(\eta^5\text{-Cp})Mn(CO)_3]$ the calculated geometry (with C_s symmetry) is compared with a high-precision X-ray determination performed at low temperature [58]. Both correspond to an almost perfect planar η^5-Cp with Mn–C distances very similar for the five carbon atoms (2.14 Å for the experimental structure and 2.22 Å for the optimised complex). The calculated C–O distances are also slightly longer than the experimental ones (1.18 Å for the optimised geometry and 1.15 Å for the mean value of the crystal structure), the remaining structural parameters being in the range of the experimental values. This pattern repeats itself for all the complexes studied.

The coordination mode for the ligands with one benzene ring fused to the C_5 bonding ring, the indenyl and indacene complexes, exhibits a small distortion in the Mn–C_5 bond lengths, as shown by both the calculated (around 2.2 Å for carbons a, b and b′; and 2.3 for the two hinge carbons, c and c′) and the experimental distances (2.1 Å for C_a, C_b and $C_{b'}$; and 2.2 Å for C_c and $C_{c'}$). The same happens with the larger ligands, flu and cpp, with two and three benzene rings fused to the C_5 pentagon directly bonded to the metal. For these, the calculated and experimental Mn–C_x distances are, respectively: 2.2 and 2.1 Å for carbon a; 2.3 and 2.2 Å for carbons b and b′; 2.3 and 2.2 Å for carbons c and c′. This is due to the nodal characteristics of the ligands π orbitals involved in the (η^5-X)–Mn bonding. Namely, the loss of symmetry that happens in going from Cp to the larger ligands, breaks the degeneracy between the $2\pi_s$ and $1\pi_a$ ligands orbitals (Fig. 1) with the conse-

quent non equivalence of the X–M interactions, π_s and π_a. This was shown for indenyl complexes [54], were a $\eta^3 + \eta^2$ coordination rather than a pure η^5 is proposed for these cases.

However, some conclusions can still be drawn comparing the (η^5-X)–Mn bonding in the different complexes, if the structural parameters of Table 1 are carefully analysed. The experimental and theoretical values of the Mn–C mean distances for the bonded C_5 ring are presented in Table 2 for the hydrocarbon polyenic complexes studied, as well as the corresponding $(\eta^5\text{-X})^-$–$[Mn(CO)_3]^+$ extended Hückel (EH) overlap populations (OPs). Both the experimental and the theoretical distances show a consistent increase with polyenic π system extension.

Thus, Cp has the shortest mean Mn–C bond distances (2.14 and 2.22 Å for the experimental and the theoretical values, respectively), followed by the ligands with one fused benzene ring, indenyl and indacene, 2.16 Å (experimental) and 2.25 Å (theoretical), the longest distances belonging to the larger flu and cpp ligands, with two and three fused benzene, 2.19 Å (experimental) and 2.28 Å (theoretical).

An electronic reason must be behind this result, since the EH overlap populations, calculated for model complexes with the same Mn–C distances (see Appendix for details), diminish with increasing ligand complexity. The highest OP is found for the Cp complex, [(η^5-Cp)$Mn(CO)_3$] (0.62), followed by the indenyl and indacene complexes (0.53), the flu and cpp species presenting the lowest value (0.48).

In fact, when a Cp ring is coordinated to a metal in a η^5 mode, its entire π system is involved in the bonding, with all the five carbon atoms directly bonded to the metal. This means that the relevant ligand orbitals ($1\pi_s$, $2\pi_s$ and $1\pi_a$) effectively use all the electron density for the interaction with the metal. On the other hand, for the larger ligands only a part of the π system atoms is directly bonded to the metal, and, consequently, only a fraction of the electron density of the ligand orbitals is effectively used, resulting in a weaker interaction. This effect is clear from the comparison of the two extreme examples, the Cp and the cpp complexes, where the difference is bigger and its causes easier to trace. Let us take, for example, the more symmetrical ligand orbital, $1\pi_s$, involved in the (η^5-X)–Mn σ interaction (cf. Fig. 1). In the case of Cp, the five carbon atoms bonded to the metal bear the totality of its electron density, on the other hand, for cpp the atoms of the C_5 ring have only 59% of the orbital electron density. The weakening of the σ interaction, can be spotted by bond strength indicators, such as the OPs between the fragment molecular orbitals (FMOs) involved in the σ interaction, 0.15 for the Cp complex and 0.07 for cpp, or the electronic population of the ligands $1\pi_s$ orbital in the complexes, 1.862 and 1.935 electrons for the Cp and the cpp complexes, respectively. As the polyenic bonding results formally from X to metal donations, a stronger interaction corresponds to a less populated ligand orbital in the complex.

Table 2
Comparation between the (η^5-X)–Mn bond for the hydrocarbon polienyl complexes, [(η^5-X)$Mn(CO)_3$]

X	$\langle d_{M-C}\rangle$/Å (exp)	$\langle d_{M-C}\rangle$/Å (theor)	OP{$(\eta^5\text{-X})^-$–$[Mn(CO)_3]^+$}
Cp	2.14	2.22	0.624
Ind	2.16	2.25	0.534
as-ind	2.16	2.25	0.529
s-ind	2.16	2.25	0.529
flu	2.19	2.28	0.476
cpp	2.19	2.28	0.475

In spite of the subtle differences presented by the (η^5-X)–Mn bonding for the different polyenic complexes, the other half of the molecule remains curiously similar for all of them. In fact, the Mn–(CO) bonding is similar for the studied species, as shown by the Table 1 values. The Mn–C(CO) distances are around 1.79 Å for both the calculated and the experimental structures, the C–O bonds, are equivalent for the different complexes (1.15 and 1.18 Å for the experimental and calculated values, respectively), and the X–Mn–CO angles (α in Scheme 3) do not change from one complex to another, the calculated values, 123–124°, being in excellent agreement with the experimental values. This shows that the electronic structure in the complexes is indeed similar, and the discussed differences in the polyenic bonding are small enough not to affect the remaining fragment of the molecule.

An absolute agreement is found between the more stable conformations (I or II, in Scheme 3) of the optimised geometries, and the experimental structures. Of all the hydrocarbon polyenic species, only for X = flu or cpp is the alternating conformation, II, preferred, but, as small energy differences were obtained for the two conformations, $\leq$ 0.16 eV for the all species, facile rotations are expected. This seams to indicate that stereochemical reasons are behind the preferred conformation, since there is a clear dependence on the polyenic ligand geometrical shape, and no electronic reason was found after an orbital analysis.

2.2. Complexes with η^3-coordinated polyenic ligands, $[(\eta^3\text{-X})Mn(CO)_3]^{2-}$

The haptotropic shift resulting from a η^5 to η^3 change in the coordination mode of a polyenic ligand has been studied for indenyl complexes, and the reasons behind the well-known η^3 folded indenyl coordination fully discussed [16–18,21,54]. In fact, the effect of a two-electron addition on the (η^5-X)–Mn bond of an 18-

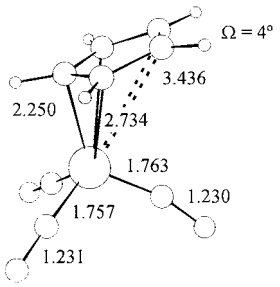

Fig. 2. Optimised geometry of $[(\eta^3\text{-Cp})Mn(CO)_3]^{2-}$, with the more relevant structural parameters (distances in Å).

electron complex with a C_5 ring can be explained with the help of the diagram from Fig. 1. The extra electrons will occupy the π_s^* (η^3-X)–Mn antibonding orbital, the LUMO of the η^5 complex. The occupation of an antibonding orbital forces the η^5 to η^3 structural rearrangement normally called ring slippage. Namely, the reduced species is stabilised by the partial relief of the antibonding character of π_s^*, the η^3 complex HOMO. From the geometrical point of view, this is accomplished by the elongation of the Mn–C bond lengths for the two hinge carbons (c and c′), beyond bonding distances. This results in the typical η^3 folded coordination modes of the indenyl complexes, with M–C distances of 3.0 Å or higher for the hinge carbons and the corresponding folding angles Ω that can be as high as 30° [54]. Ligands with more rigid C_5 rings, such as fluorenyl or cpp, are known to adopt a different η^3 coordination geometry, binding in an *exo*cyclic way (see Scheme 1) in which the relieving of the antibonding character of the corresponding π_s^* orbital is still more efficient, since there are no hinge carbons. Another argument often proposed to explain the stabilisation of the η^3 species is the creation of aromaticity in the uncoordinated portion of the ligands, as the benzene ring of η^3-Ind or the more extensive π systems of flu and cpp.

In this work, the η^3 species resulting from a two-electron reduction of the parent $[(\eta^5\text{-X})Mn(CO)_3]$ complexes are studied, the geometries optimised and the (η^3-X)–Mn bond discussed, in each case. All the geometries obtained for the reduced species, $[(\eta^3\text{-X})Mn(CO)_3]^{2-}$, are the result of full optimisations, starting from the corresponding η^5 complexes.

The optimised geometry for the Cp complex, $[(\eta^3\text{-Cp})Mn(CO)_3]^{2-}$, is shown on Fig. 2, with the more relevant structural parameters. This complex presents an almost planar Cp as shown by the folding angle, $\Omega = 4°$, and, hence, the resulting coordination mode is closer to η^1 than to η^3, the Mn–C distances to carbons b and b′ being quite long (2.73 Å). The apex carbon, C_a, lies at 2.25 Å from the metal, this value being close to the corresponding bond lengths obtained for the η^5 complex (2.22 Å). The two hinge carbons, C_c and $C_{c'}$, are far beyond bonding distances (Mn–C = 3.44 Å).

This Cp preference to slip rather than fold is due to the maintenance of the ring aromaticity, which would be lost if a clear folded η^3 coordination was adopted. The electronic nature of this coordination geometry is corroborate by EH calculations on model complexes. The relevant overlap populations are 0.209 for $(\eta^3\text{-Cp})^-$–$[Mn(CO)_3]^-$ and 0.258 for $(\eta^1\text{-Cp})^-$–$[Mn(CO)_3]^-$, showing that a perfectly planar η^1-Cp results in a stronger bond to the metal, the corresponding complex being 0.9 eV more stable. Although the only X-ray structure available for a η^3-Cp complex [13] shows a quite bent Cp ($\Omega = 20°$), it refers to a bis-Cp complex, $[Cp_2W(CO)_2]$, with a completely different metal centre, not being directly comparable with the system studied in this work.

Both the optimised structures for the η^3-reduced complexes of the two larger ligands, flu and cpp, present the *exo*cyclic coordination mode (see Fig. 3). In fact, even starting from a perfect η^5 coordination, no local minimum was found for the *endo*cyclic η^3 coordination of those ligands (cf. Scheme 1).

The Mn–C bond lengths presented in Fig. 3 for both complexes are within bonding values, being around 2.2 Å for the apex carbon and between 2.3 and 2.5 Å for the side ones. However, a closer look at these structural parameters shows a somewhat surprising result, as for the cpp complex the Mn–C bonds are shorter than for the flu species (the Mn–C mean distance is 2.33 for cpp and 2.38 Å for flu). This is the opposite of what would

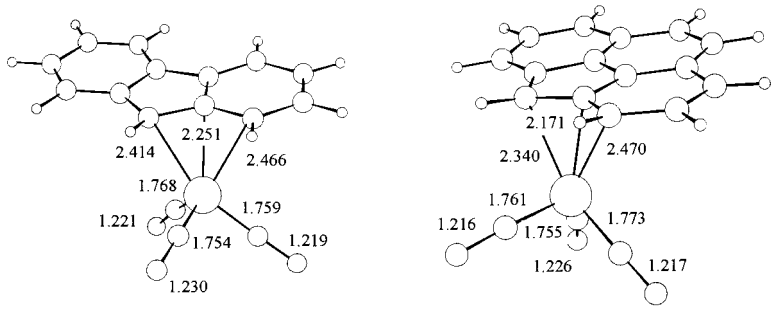

Fig. 3. Optimised structures of $[(\eta^3\text{-flu})Mn(CO)_3]^{2-}$ (left) and $[(\eta^3\text{-cpp})Mn(CO)_3]^{2-}$ (right), with the more relevant bond lengths (Å).

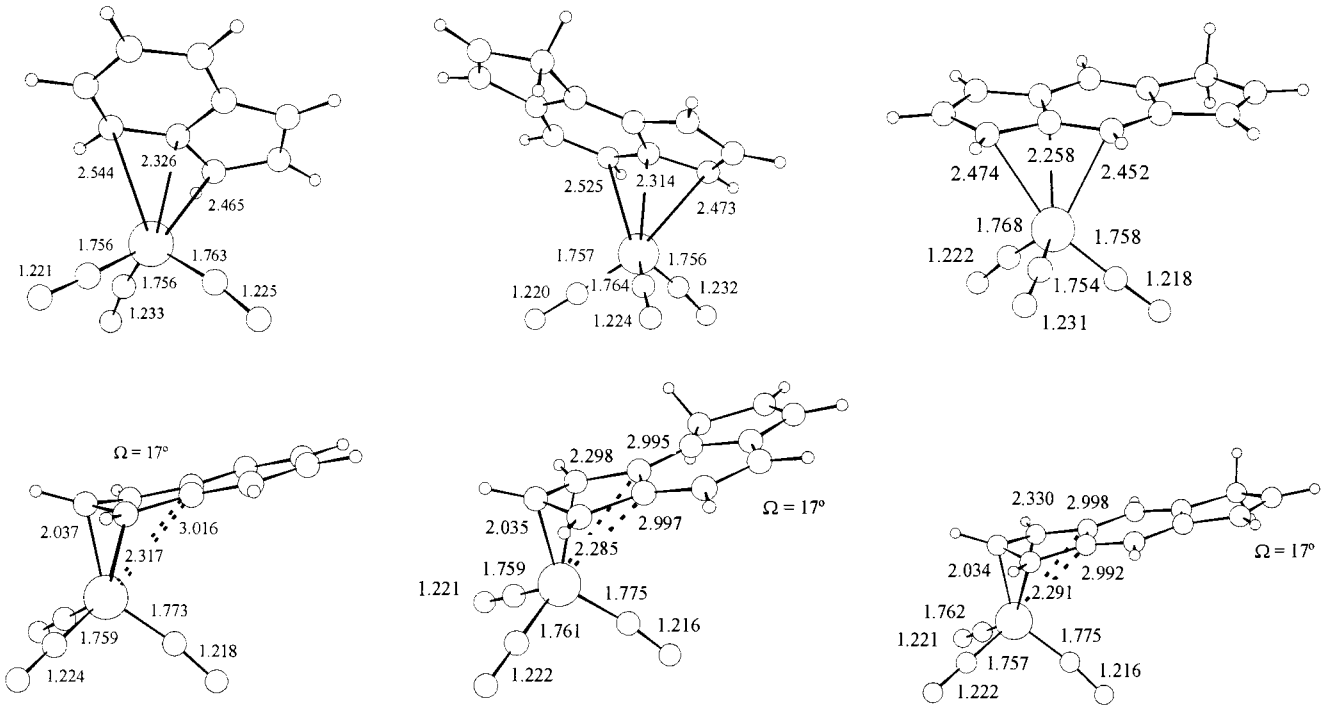

Fig. 4. Optimised structures of $[(\eta^3\text{-X})Mn(CO)_3]^{2-}$ for X = Ind (left), *as*-ind (centre) and *s*-ind (right), in the *exo*cyclic (top) and *endo*cyclic (bottom) coordination. The more relevant bond lengths (Å) are presented.

be expected from stereochemical arguments, cpp being the larger ligand. In addition, the electronic reasoning used to explain the X–Mn bonding in the η^5 complexes does not apply here, because cpp has a wider π system.

In spite of the small difference, an electronic reason was sought by means of EH calculations on the appropriate model complexes, $[(\eta^3\text{-flu})Mn(CO)_3]^{2-}$ and $[(\eta^3\text{-cpp})Mn(CO)_3]^{2-}$, with the same Mn–C distances. The results yielded a slightly stronger bond in the cpp case, in accordance with the distances found in the optimised structures, as shown by the following OPs: 0.255 for $(\eta^3\text{-flu})^-$–$[Mn(CO)_3]^-$ and 0.275 for $(\eta^3\text{-cpp})^-$–$[Mn(CO)_3]^-$. The reason lies in the X–Mn π_a interaction as indicated by the FMO OP for this interaction (0.08 for flu and 0.10 for cpp), and it is due to the nodal characteristics of the ligand $1\pi_a$ orbital involved. In fact, for cpp 54% of the electronic density of this orbital sits on the three carbons bonded to the metal, for flu being only 49%. Thus, the $1\pi_a$ orbital of cpp is effectively more involved in the interaction with the metal, resulting in a stronger bond.

For the ligands X with one fused benzene ring, indenyl and indacene, two possible η^3 coordination geometries were studied (see Scheme 1), the *endo*cyclic folded coordination, well known for indenyl complexes, and the allylic *exo*cyclic mode, parallel to what is found in the flu and cpp complexes. In fact, on the grounds of a simple orbital explanation for the η^5 to η^3 shift, such as the partial relief of the π_s^* X–M interaction, the *exo*cyclic geometry should be more effective. In this case, a completely η^3 coordination is accomplished, since there are no hinge carbons in the metal neighbourhood, instead of the plain C_c and $C_{c'}$ separation of the folded *endo*cyclic mode. However, all the structural characterised η^3-Ind complexes exhibit the folded coordination mode, and, to our knowledge, there are no examples of allylic *exo*cyclic geometries. The creation of an aromatic benzene in the latter species is usually pointed out as an additional stabilising factor, and can make the difference between the two possible coordination modes.

The optimised geometries of the η^3 complexes for the three ligands (Ind, *as*-ind and *s*-ind) in the two coordination modes are shown in Fig. 4 with the relevant bond lengths. In each case, an almost complete equivalence is found between the different ligands.

Nearly planar ligands were obtained for the *exo*cyclic structures, with the three allylic carbons at bonding distances from the metal, around 2.3 Å for the central carbon and 2.5 Å for the side ones. On the other hand, the *endo*cyclic complexes have clearly folded ligands, with folding angles $\Omega = 17°$ in all cases, the Mn–C distances being approximately 2.0 for C_a, 2.3 for $C_{b,b'}$, and 3.0 Å, outside the bonding range, for C_c and $C_{c'}$. These values compare well with the ones found in the X-ray crystal structure of $[(\eta^3\text{-Ind})Fe(CO)_3]^-$ [29], isoelectronic with the indenyl complex of the present work, the tendency for slightly longer calculated M–C distances, found for the η^5 complexes, being maintained: Fe–C_a = 1.996 Å, Fe–C_b = 2.183 Å, Fe–$C_{b'}$ =

2.192 Å, Fe–C_c = 2.885 Å, Fe–$C_{c'}$ = 2.869 Å and Ω = 22° (cf. Fig. 4 for a more accurate comparison with the Ind complex).

All the previous complexes present a clear preference for the folded *endo*cyclic η^3 coordination mode, as this is always the more stable of the two optimised geometries of the $[(\eta^3\text{-X})Mn(CO)_3]^{2-}$ complexes (0.41 eV for X = Ind, 0.48 eV for X = *as*-ind and 0.45 eV for X = *s*-ind). The mean Mn–C distances, to the three bonding carbons are also shorter for the folded coordination (2.2 vs. 2.4 Å in the *exo*cyclic mode), indicating a stronger X–Mn bond. EH calculations were performed on $[(\eta^3\text{-Ind})Mn(CO)_3]^{2-}$ model complexes with the two coordination modes, in order to study the Ind–Mn bond and help explaining the differences. A simplified MO diagram for the (η^3-Ind)–Mn bonding is presented in Fig. 5 for the two coordination modes.

The three interactions already found for the η^5 molecules, σ, π_s and π_a (Fig. 1), can be seen in Fig. 5, being the basis of the bonding in the η^3 species, for both coordination geometries. The main difference is that for the η^5 complexes only the bonding MOs were filled, and, in the reduced species, one of the antibonding orbitals (π_s^*) is filled, the HOMO of the $[(\eta^3\text{-Ind})Mn(CO)_3]^{2-}$ complexes. The net result is the formation of two bonds, both Ind to metal donations. The relieving of the Mn–X antibonding character of π_s^* is the driving force for the hapticity change from η^5 to η^3. This is true for the *exo*cyclic, as well as for the *endo*cyclic, or folded, coordination mode of the indenyl ligands of Fig. 5.

The EH results are in good agreement with the ab initio calculations, also pointing towards a more stable *endo*cyclic complex (by 0.2 eV) due to a stronger (η^3-

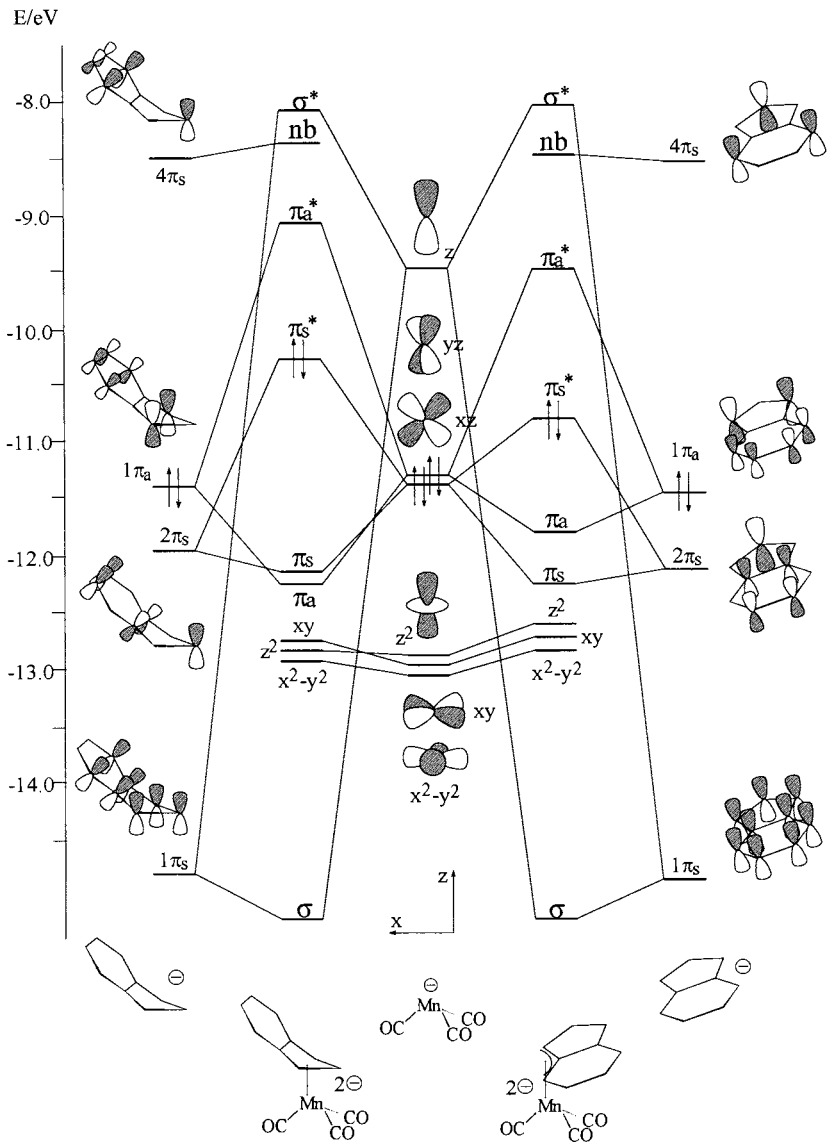

Fig. 5. Simplified MO diagram for the interaction between $[Mn(CO)_3]^-$ (central) and an *endo*cyclic (left) or an *exo*cyclic (right) η^3-Ind^-.

Ind)$^-$–[Mn(CO)$_3$]$^-$ bond, the corresponding OPs being 0.219 for the *exo*, and 0.311 for the *endo*cyclic coordination. Nevertheless, a more efficient relieving of the HOMO, π_s^*, (η^3-Ind)–Mn antibonding character is obtained in the *exo*cyclic geometry, that orbital being 0.5 eV more stable than the *endo*cyclic analogue (cf. Fig. 5). As predicted by qualitative considerations, the absence of the hinge carbons greatly stabilises that orbital in the *exo*cyclic species when compared with the increase of the Mn–$C_{c,c'}$ distances that occurs in a η^3 folded complex. The preference for the *endo*cyclic coordination has to be traced elsewhere.

The main difference between the bonding in the two [(η^3-Ind)Mn(CO)$_3$]$^{2-}$ complexes is the strength of the π_a interaction, which is considerably stronger in the *endo*cyclic case, as shown by the FMO OPs (0.17 vs. 0.30). Although the same indenyl orbital ($1\pi_a$) is used for this interaction in both geometries, the overlap with the metal orbitals is poorer in the *exo*cyclic complex. This is due to the nodal characteristics of that orbital, in which most of the electronic density (60%) lies on the three carbon atoms connected to the metal in a *endo*-cyclic geometry, but only 43% belong to the bonding atoms of an *exo*cyclic indenyl.

In short, there are two opposite effects in the η^5 to η^3 structural distortion, resulting from an increase on the metal electron counting in a polyenic complex, such as the ones discussed here. On one hand, it relieves the X–M antibonding character of an orbital (π_s^*) that becomes occupied on the reduced complex, this being the haptotropic rearrangement driving force. On the other hand, it produces the weakening of the M–X bonding interactions, as some Mn–C bonds are broken. The preferred η^3 coordination geometry is the result of a compromise between these two factors. For the studied indenyl and indacene complexes, [(η^3-X)Mn(CO)$_3$]$^{2-}$, although the HOMO stabilisation is more effective in an *exo*cyclic geometry, the losses in the bonding interactions overtake this effect and the more stable coordination mode is the *endo*cyclic with a folded η^3-X, well known for the indenyl complexes.

The Mn–CO bonding is quite similar for all the optimised η^3 complexes, as shown by the obtained geometries (Figs. 2–4). This parallels what was found for η^5 neutral species, although in this case the results are more uniform, as the same coordination mode was present for all complexes. The (η^3-X)–Mn bonding does not seem to have a direct effect on the bonds of the remaining fragment of the molecule, any more than in the η^5 species, previously discussed.

Yet, some conclusions can be drawn from the comparison of the carbonyl bond lengths on the [(η^3-X)Mn(CO)$_3$]$^{2-}$ complexes, with the corresponding values obtained for the parent η^5 neutral species. For the latter, the calculated Mn–C(CO) bond lengths were 1.79 Å and the C–O distance 1.18 Å (see Table 1). On the other hand, for the reduced complexes, those values are around 1.76–1.77 and 1.22–1.23 Å, respectively. This shows a clear increase on the C–O bond distance and a shortening of the Mn–C with the reduction, and can be explained by an increase on the Mn to carbonyl backdonation to a CO π^* orbital, with the consequent strengthening of the Mn–C bond and weakening of the C–O, resulting from the partial occupation of an antibonding orbital. The EH results on the [(η^3-Ind)Mn(CO)$_3$]$^{2-}$ *endo*cyclic model corroborate this conclusion, since the corresponding HOMO (Fig. 6) clearly shows metal d to carbonyl π^* backdonation. In fact, 18% of that orbital is due to the contribution from the carbonyl π^* orbitals.

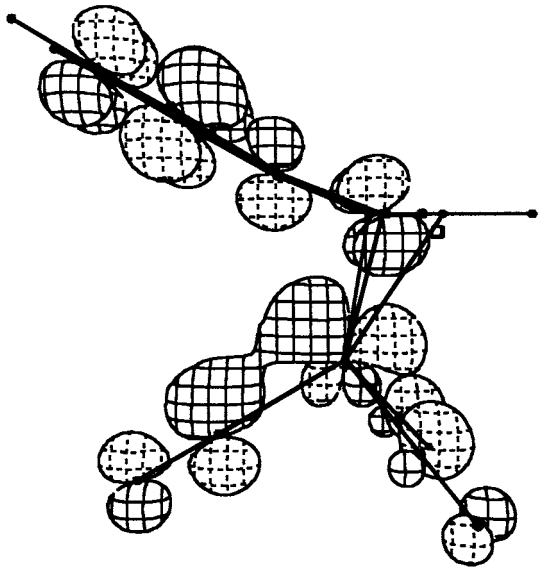

Fig. 6. 3D representation of the [(η^3-Ind)Mn(CO)$_3$]$^{2-}$ HOMO (π_s^*).

Although no attempt was made to follow the reaction path or determine the transition state corresponding to the [(η^5-X)Mn(CO)$_3$] + 2e → [(η^3-X)Mn(CO)$_3$]$^{2-}$ reduction, some conclusions may be drawn on the ease of the haptotropic shift by looking at the energy difference, $\Delta E = E(\eta^5 \text{ complex}) - E(\eta^3 \text{ complex})$, obtained for the η^5 and η^3 complexes, in each case. The results ($\Delta E = 2.74$ eV for Cp, 1.21 eV for Ind, 0.54 eV for *as*-ind, 0.49 for *s*-ind, 0.72 eV for flu and -0.01 eV for cpp) seem to suggest an increasing ease of the ring slippage with the ligand's π-system extension.

2.3. Complexes with heterocyclic ligands, X = pyr and tp

The structural parameters obtained for the optimised geometries of the heterocyclic complexes, [(η^5-pyr)Mn(CO$_3$)] and [(η^5-tp)Mn(CO$_3$)]$^+$, are presented in Table 1. The values are in reasonable agreement with the experimental X-ray structures, since these be-

long to complexes with substituted ligands. Thus, the discussion presented for the corresponding hydrocarbon polyenic ligands holds for the two heterocyclic complexes.

A comparison of the X–Mn bonding in the two complexes seems to point towards a stronger bond for the nitrogen ligand, with shorter mean bonding distances from the metal to the ligand's five atoms. The experimental and theoretical values (Å) are, respectively, 2.13 and 2.23 for the pyr complex, and 2.23 and 2.37 for the tp species. There is an electronic reason behind this result, reflecting the donor abilities of the two heteroatoms, N and S, since the EH OPs calculated on model complexes show the same trend: 0.572 for (η^5-pyr)–$[Mn(CO)_3]^+$ and 0.543 for (η^5-tp)$^-$–$[Mn(CO)_3]^+$.

The effect of a two-electron reduction on those complexes was analysed, in a similar way to that previously described for the hydrocarbon ligand complexes. The geometries of the reduced species, $[(pyr)Mn(CO_3)]^{2-}$ and $[(tp)Mn(CO_3)]^-$, were obtained, by full optimisations, starting from the η^5 complexes. No local minimum was found for a slipped or folded η^3 coordination of either the heterocyclic ligands. Both the obtained pyr and the tp reduced complexes present σ-bonded ligands, in which the (σ − X)–Mn bond is assured by the heteroatom lone pair, pointing towards the metal. The obtained structures, and the more important bond lengths are presented in Fig. 7.

The only available X-ray structures, resulting from a CSD [11] survey, for manganese complexes with σ-pyr ligands belong to polynuclear species with the pyrrolyl bridging two metal atoms, being η^5 bonded to one Mn, through the ligand π system, and using the N lone pair to bond the other Mn in a σ fashion [67,68]. Although in those species the σ-bonded metal is an octahedral Mn(I), the experimental Mn–N distances (2.09 to 2.12 Å) compare fairly well with the calculated 2.02 Å for the $[(\sigma\text{-pyr})Mn(CO_3)]^{2-}$ molecule. It was not found in a CSD survey any σ-tp manganese complexes, the only related species found being tetrahydrothiophene complexes, not directly comparable to the complex studied.

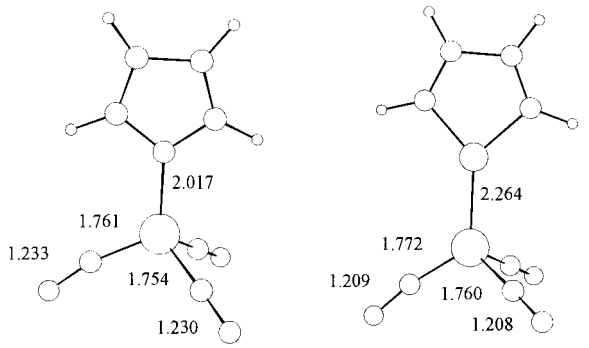

Fig. 7. Optimised structures for $[(\sigma\text{-pyr})Mn(CO_3)]^{2-}$ (left) and $[(\sigma\text{-tp})Mn(CO_3)]^-$ (right), with the more relevant bond lengths (Å).

An EH study was performed in order to help explain, through a simple orbital reasoning, the heterocyclic preference for a σ rather than an η^3 coordination. Calculations done on $[(\sigma\text{-pyr})Mn(CO_3)]^{2-}$ and $[(\eta^3\text{-pyr})Mn(CO_3)]^{2-}$ model complexes, show an additional stability for the σ-pyr species (by 1.8 eV), due to a stronger $(pyr)^-$–$[Mn(CO)_3]^-$ bond, the corresponding OP being 0.374 and 0.165, respectively.

An analysis of the (η^3-pyr)–Mn interaction shows the pattern already discussed for the η^3 *endo*cyclic coordination of the indenyl and indacene complexes (see above), with the three σ, π_s and π_a, metal–pyr interactions. The complex HOMO (π_s^*) is equivalent to the one found for the corresponding indenyl complex (Fig. 6), being the antibonding orbital for the symmetrical pyr–Mn π interaction. The η^3 coordination produces the same compromise between relieving the HOMO antibonding character and weakening of the bonding character of all the interactions, described for the indenyl complexes. On the other hand, in a σ-coordinated pyrrolyl complex, the only important pyr–Mn interaction is the one between the N lone pair and the empty metal *z* orbital, corresponding to interaction σ in Figs. 1 and 5. This means that, if a σ coordination is adopted, the metal *xz* orbital involved in the π_s interaction in a η^3 complex (see Fig. 5), will be free to accept the two extra electrons, remaining essentially pyr–Mn nonbonding. Thus, in the latter geometry, the occupation of an antibonding orbital is avoided. The higher overlap allowed by the shorter heteroatom to metal bond lengths is another important stabilising factor in the σ complexes: Mn–N = 2.22 Å (η^5) and 2.02 Å (σ); Mn–S = 2.54 Å (η^5) and 2.26 Å (σ).

Although the Mn–CO bond lengths show a less effective backdonation for thiophene complexes due to the overall charge of the complex, the changes on the Mn–C(CO) and C–O distances, discussed above for the hydrocarbon ligands, are also found going from the η^5 to the reduced heterocyclic complexes (cf. Table 1 and Fig. 7).

3. Conclusions

A slight weakening of the X–Mn bond with the increasing of the polyenic ligand's π-system extension, was found for the $[(\eta^5\text{-X})Mn(CO_3)]$ complexes. This is related with the fraction of ligands atoms involved in the conjugated system, actually bonded to the metal. In fact, the larger the ligand, the smaller will be the fraction corresponding to the five atoms connected to the metal in a η^5-X complex. Consequently, the fraction of the ligand's orbitals electronic density effectively involved in the interaction with the metal will be smaller, resulting in a weaker bond.

The η^5–η^3 haptotropic shifts in polyenic complexes result from the relieving of electronic density excess on the metal atom. Using orbital arguments, that structural change is driven by the stabilisation of an X–M antibonding orbital that becomes occupied when there is a two-electron addition to the η^5 complex.

All the hydrocarbon polyenic complexes studied present η^5–η^3 ring slippage after a two-electron reduction. However, only the ones having rigid C_5 ring and large π systems, the fluorenyl and cpp (cyclopenta[*def*]phenanthrenyl) species, show preference for an η^3 *exo*cyclic coordination. The ligands with flexible C_5 rings, such as the indenyl and indacene complexes, adopt folded *endo*cyclic η^3 geometries, since a stronger overall X–M interaction is obtained.

The pyrrolyl and thiophene reduced complexes have σ-bonded ligands, the X–M bond being achieved through the heteroatom lone pair pointing towards the metal.

Acknowledgements

The author gratefully acknowledges Professors M.J. Calhorda and C.C. Romão for introducing him to this subject, Professor A.R. Dias for helpful discussions and Dr M.F. Minas da Piedade for help with the CSD. Praxis XXI is acknowledged for partial funding of this work.

Appendix

Geometry optimisations were accomplished by means of ab initio calculations performed with the GAUSSIAN 98 program [69]. The B3LYP hybrid functional with a LANL2DZ basis set was used in all calculations. That functional includes a mixture of Hartree–Fock [70] exchange with DFT [71] exchange-correlation, given by Becke's three-parameter functional [72] with the Lee, Yang and Parr correlation functional, which includes both local and non-local terms [73,74].

For the η^5 complexes, partial optimisations were performed in which all atoms bonded to the metal were allowed to adjust their positions. Namely, the Mn–C–O angles were frozen at 180°, and the C–H distances at 1.08 Å. The polyenic portions not bonded to the metal were maintained planar. The η^3 intermediates resulted from full geometry optimisations. C_s symmetry was used whenever possible. Unrestricted calculations performed on η^3 complexes failed to yield triplet species more stable than the singlet ground-state geometries presented.

The extended Hückel calculations [55,56] were done with the CACAO program [75] and modified H_{ij} values were used [76]. The basis set for the metal atoms consisted of *n*s, *n*p and (*n*-1)d orbitals. The s and p orbitals were described by single Slater-type wave functions, and the d orbitals were taken as contracted linear combinations of two Slater-type wave functions. Only s and p orbitals were considered for S. The parameters used for Mn were the following (H_{ii} (eV), ζ): 4s −9.880, 1.800; 4p −5.450, 1.800; 3d −12.530, 5.150, 1.900 (ζ_2), 0.5311 (C_1), 0.6479 (C_2). Standard parameters were used for other atoms. Calculations were performed on models based on the optimised geometries with idealised maximum symmetry, and the following distances (Å) and angles (°): Mn–C_5 (centroid) 1.77, Mn–C (CO) 1.80, Mn–N (σ-pyr) 2.00, Mn–S (σ-tp) 2.00, C–O 1.15, C–C 1.40, C–N 1.40, C–S 1.40, C–H 1–08, X–Mn–CO 120.0.

References

[1] J.M. O'Connor, C.P. Casey, Chem. Rev. 87 (1987) 307.
[2] M.E. Rerek, L.-N. Ji, F. Basolo, J. Chem. Soc. Chem. Commun. (1983) 1208.
[3] T.B. Marder, D.C. Roe, D. Milstein, Organometallics 7 (1988) 1451.
[4] A. Borrini, P. Diversi, G. Ingrosso, A. Lucherini, G. Serra, J. Mol. Catal. 30 (1985) 181.
[5] H. Bönnemann, Angew. Chem. Int. Ed. Engl. 24 (1985) 248.
[6] T. Foo, R.G. Bergman, Organometallics 11 (1992) 1801.
[7] M.A. Schmid, H.G. Alt, W. Milius, J. Organomet. Chem. 514 (1996) 45.
[8] G.H. Llinas, R.O. Day, M.D. Rausch, J.C.W. Chien, Organometallics 12 (1993) 1283.
[9] C.E. Garrett, G.C. Fu, J. Org. Chem. 63 (1998) 1370.
[10] L.-N. Ji, M.E. Rerek, F. Basolo, Organometallics 3 (1984) 740.
[11] F.H. Allen, J.E. Davies, J.J. Galloy, O. Johnson, O. Kennard, C.F. Macrae, D.G. Watson, J. Chem. Inf. Comp. Sci. 31 (1991) 204.
[12] W. Simanko, V.N. Sapunov, R. Schmid, K. Kirchner, S. Wherland, Organometallics 17 (1998) 2391.
[13] G. Huttner, H.H. Britzinger, L.G. Bell, P. Frieddrich, V. Bejenke, D. Neugebauer, J. Organomet. Chem. 141 (1978) 329.
[14] G.A. Miller, M.J. Therien, W.C. Trogler, J. Organomet. Chem. 383 (1990) 271.
[15] J.R. Ascenso, C.G. Azevedo, I.S. Gonçalves, E. Herdtweck, D.S. Moreno, M. Pessanha, C.C. Romão, Organometallics 14 (1995) 3901.
[16] M.J. Calhorda, V. Félix, C.A. Gamelas, I.S. Gonçalves, C.C. Romão, L.F. Veiros, to be submitted.
[17] M.J. Calhorda, C.A. Gamelas, I.S. Gonçalves, E. Herdtweck, J.P. Lopes, C.C. Romão, L.F. Veiros, XIIth FECHEM, Prague, Czech Republic, 1997.
[18] M.J. Calhorda, V. Félix, C.A. Gamelas, I.S. Gonçalves, C.C. Romão, L.F. Veiros, XVII Reunión del Grupo Especializado de Química Organometálica, Barcelona, Spain, 1998.
[19] S. Lee, S.R. Lovelace, N.J. Cooper, Organometallics 14 (1995) 1974.
[20] C. Amatore, A. Ceccon, S. Santi, J.-N. Verpeaux, Chem. Eur. J. 3/2 (1997) 279.
[21] M.J. Calhorda, C.A. Gamelas, I.S. Gonçalves, E. Herdtweck, C.C. Romão, L.F. Veiros, Organometallics 17 (1998) 2597.
[22] L.-N. Ji, M.E. Rerek, F. Basolo, Organometallics 3 (1984) 740.
[23] R.M. Kowalewski, A.L. Rheingold, W.C. Trogler, F. Basolo, J. Am. Chem. Soc. 108 (1986) 2460.

[24] Z. Zhou, C. Jablonski, J. Brisdon, J. Organomet. Chem. 461 (1993) 215.
[25] R.N. Biagioni, A.D. Luna, J.L. Murphy, J. Organomet. Chem. 476 (1994) 183.
[26] D.A. Brown, N.J. Fitzpatrick, W.K. Glass, H.A. Ahmed, D. Cunningham, P. McArdle, J. Organomet. Chem. 455 (1993) 157.
[27] K.A. Pevear, M.M. Banaszak Holl, G.B. Carpenter, A.L. Rieger, P.H. Rieger, D.A. Sweigart, Organometallics 14 (1995) 512.
[28] J.S. Merola, R.T. Kacmarcik, D. Van Engen, J. Am. Chem. Soc. 108 (1986) 329.
[29] T.C. Forschner, A.R. Cutler, R.K. Kullnig, Organometallics 6 (1987) 889.
[30] R. Poli, S.P. Mattamana, L.R. Falvello, Gazz. Chim. Ital. 122 (1992) 315.
[31] J.R. Ascenso, C.G. Azevedo, I.S. Gonçalves, E. Herdtweck, D.S. Moreno, C.C. Romão, J. Zühlke, Organometallics 13 (1994) 429.
[32] I.S. Gonçalves, C.C. Romão, J. Organomet. Chem. 486 (1995) 155.
[33] J.W. Faller, R.H. Crabtree, A. Habib, Organometallics 4 (1985) 929.
[34] J.W. Faller, C.-C. Chen, M.J. Mattina, A. Jakubowski, J. Organomet. Chem. 52 (1973) 361.
[35] T.A. Huber, F. Bélanger-Gariépy, D. Zargarian, Organometallics 14 (1995) 4997.
[36] T.A. Huber, M. Bayrakdarian, S. Dion, I. Dubuc, F. Bélanger-Gariépy, D. Zargarian, Organometallics 16 (1997) 5811.
[37] R.H. Crabtree, C.P. Panell, Organometallics 3 (1984) 1727.
[38] T.B. Marder, J.C. Calabrese, D.C. Roe, T.H. Tulip, Organometallics 6 (1987) 2012.
[39] R.N. Biagioni, I.M. Lorkovic, J. Skelton, J.B. Hartung, Organometallics 9 (1990) 547.
[40] M.E. Rerek, F. Basolo, Organometallics 3 (1984) 647.
[41] A. Decken, J.F. Britten, M.J. McGlinchey, J. Am. Chem. Soc. 115 (1993) 7275.
[42] A. Decken, S.S. Rigby, L. Girard, A.D. Bain, M.J. McGlinchey, Organometallics 16 (1997) 1308.
[43] G.M. Diamond, M.L.H. Green, P. Mountford, N.A. Popham, A.N. Chernega, J. Chem. Soc. Chem. Commun. (1994) 103.
[44] M. Bochmann, S.J. Lancaster, M.B. Hursthouse, M. Mazid, Organometallics 12 (1993) 4718.
[45] M.J. Calhorda, I.S. Gonçalves, E. Herdtweck, C.C. Romão, B. Royo, L.F. Veiros, Organometallics, accepted for publication.
[46] T.A. Albright, P. Hofmann, R. Hoffmann, C.P. Lillya, P.A. Dobosh, J. Am. Chem. Soc. 105 (1983) 3396.
[47] A.K. Kakkar, N.J. Taylor, J.C. Calabrese, W.A. Nugent, D.C. Roe, E.A. Connaway, T.B. Marder, J. Chem. Soc. Chem Commun. (1989) 990.
[48] D. O'Hare, J.C. Green, T.B. Marder, S. Collins, G. Stringer, A.K. Kakkar, N. Kaltsoyannis, A. Kuhn, R. Lewis, C. Mehnert, P. Scott, M. Kurmoo, S. Pugh, Organometallics 11 (1992) 48.
[49] N.S. Crossley, J.C. Green, A. Nagy, G. Stringer, J. Chem. Soc. Dalton Trans. (1989) 2139.
[50] T.M. Frankcom, J.C. Green, A. Nagy, A.K. Kakkar, T.B. Marder, Organometallics 12 (1993) 3688.
[51] J.C. Green, R.P.G. Parkin, X. Yang, A. Haaland, W. Scherer, M. Tapifolsky, J. Chem. Soc. Dalton Trans. (1997) 3219.
[52] C.N. Field, J.C. Green, A.G.J. Moody, M.R.F. Siggel, Chem. Phys. 206 (1996) 211.
[53] C. Bonifaci, A. Ceccon, S. Santi, C. Mealli, R.W. Zoellner, R.W., Inorg. Chim. Acta 240 (1995) 541.
[54] M.J. Calhorda, L.F. Veiros, Coord. Chem. Rev. 185–186 (1999) 37.
[55] R. Hoffmann, J. Chem. Phys. 39 (1963) 1397.
[56] R. Hoffmann, W.N. Lipscomb, J. Chem. Phys. 36 (1962) 2179.
[57] T.A. Albright, J.K. Burdett, M.H. Whangbo, Orbital Interactions in Chemistry, John Wiley, New York, 1985.
[58] J. Cowie, E.J.M. Hamilton, J.C.V. Laurie, A.J. Welch, J. Organomet. Chem. 394 (1990) 1.
[59] M.B. Honan, J.L. Atwood, I. Bernal, W.A. Herrmann, J. Organomet. Chem. 179 (1979) 403.
[60] W.L. Bell, C.J. Curtis, A. Miedaner, C.W. Eigenbrot Jr., R.C. Haltiwanger, C.G. Pierpont, J.C. Smart, Organometallics 7 (1988) 691.
[61] W.L. Bell, C.J. Curtis, C.W. Eigenbrot Jr., C.G. Pierpont, J.L. Robbins, J.C. Smart, Organometallics 6 (1987) 266.
[62] Ref. taken from the CSD: A.I. Yarmolenko, S.V. Kukharenko, L.N. Novikova, N.A. Ustynyuk, F.M. Dolgushin, A.I. Yanovsky, Yu. T. Struchkov, T.G. Kaftaeva, Yu. F. Oprunenko, V.V. Strelets, Izv. Akad. Nauk SSSR Ser. Khim. (1996) 199.
[63] D.L. Kershner, A.L. Rheingold, F. Basolo, Organometallics 6 (1987) 196.
[64] J.E. Joachim, C. Apostolidis, B. Kanellakopulos, D. Meyer, K. Raptis, J. Rebizant, M.L. Ziegler, J. Organomet. Chem. 476 (1994) 77.
[65] T.A. Waldbach, P.H. van Rooyen, S. Lotz, Angew. Chem. Int. Ed. Engl. 32 (1993) 710.
[66] T.A. Waldbach, P.H. van Rooyen, S. Lotz, Organometallics 12 (1993) 4250.
[67] W.A. Herrmann, I. Schweizer, P.S. Skell, M.L. Ziegler, K. Weidenhammer, B. Nuber, Chem. Ber. 112 (1979) 2423.
[68] N.I. Pyshnograeva, V.N. Setkina, V.G. Andrianov, Y. Struchkov, D.N. Kursanov, J. Organomet. Chem. 186 (1980) 331.
[69] GAUSSIAN 98, Revision A.6, M.J. Frisch, G.W. Trucks, H.B. Schlegel, G.E. Scuseria, M.A. Robb, J.R. Cheeseman, V.G. Zakrzewski, J.A. Montgomery Jr., R.E. Stratmann, J.C. Burant, S. Dapprich, J.M. Millam, A.D. Daniels, K.N. Kudin, M.C. Strain, O. Farkas, J. Tomasi, V. Barone, M. Cossi, R. Cammi, B. Mennucci, C. Pomelli, C. Adamo, S. Clifford, J. Ochterski, G.A. Petersson, P.Y. Ayala, Q. Cui, K. Morokuma, D.K. Malick, A.D. Rabuck, K. Raghavachari, J.B. Foresman, J. Cioslowski, J.V. Ortiz, B.B. Stefanov, G. Liu, A. Liashenko, P. Piskorz, I. Komaromi, R. Gomperts, R.L. Martin, D.J. Fox, T. Keith, M.A. Al-Laham, C.Y. Peng, A. Nanayakkara, C. Gonzalez, M. Challacombe, P.M.W. Gill, B. Johnson, W. Chen, M.W. Wong, J.L. Andres, C. Gonzalez, M. Head-Gordon, E.S. Replogle, and J.A. Pople, Gaussian, Inc., Pittsburgh PA, 1998.
[70] W.J. Hehre, L. Radom, P. v.R. Schleyer, J.A. Pople, Ab Initio Molecular Orbital Theory, John Wiley, New York, 1986.
[71] R.G. Parr, W. Yang, Density Functional Theory of Atoms and Molecules, Oxford University Press, New York, 1989.
[72] A.D. Becke, J. Chem. Phys. 98 (1993) 5648.
[73] C. Lee, W. Yang, R.G. Parr, Phys. Rev. B 37 (1988) 785.
[74] B. Miehlich, A. Savin, H. Stoll, H. Preuss, Chem. Phys. Lett. 157 (1989) 200.
[75] C. Mealli, D.M. Proserpio, J. Chem. Ed. 67 (1990) 39.
[76] J.H. Ammeter, H.-J. Bürgi, J.C. Thibeault, R. Hoffmann, J. Am. Chem. Soc. 100 (1978) 3686.